Graphical Abstract

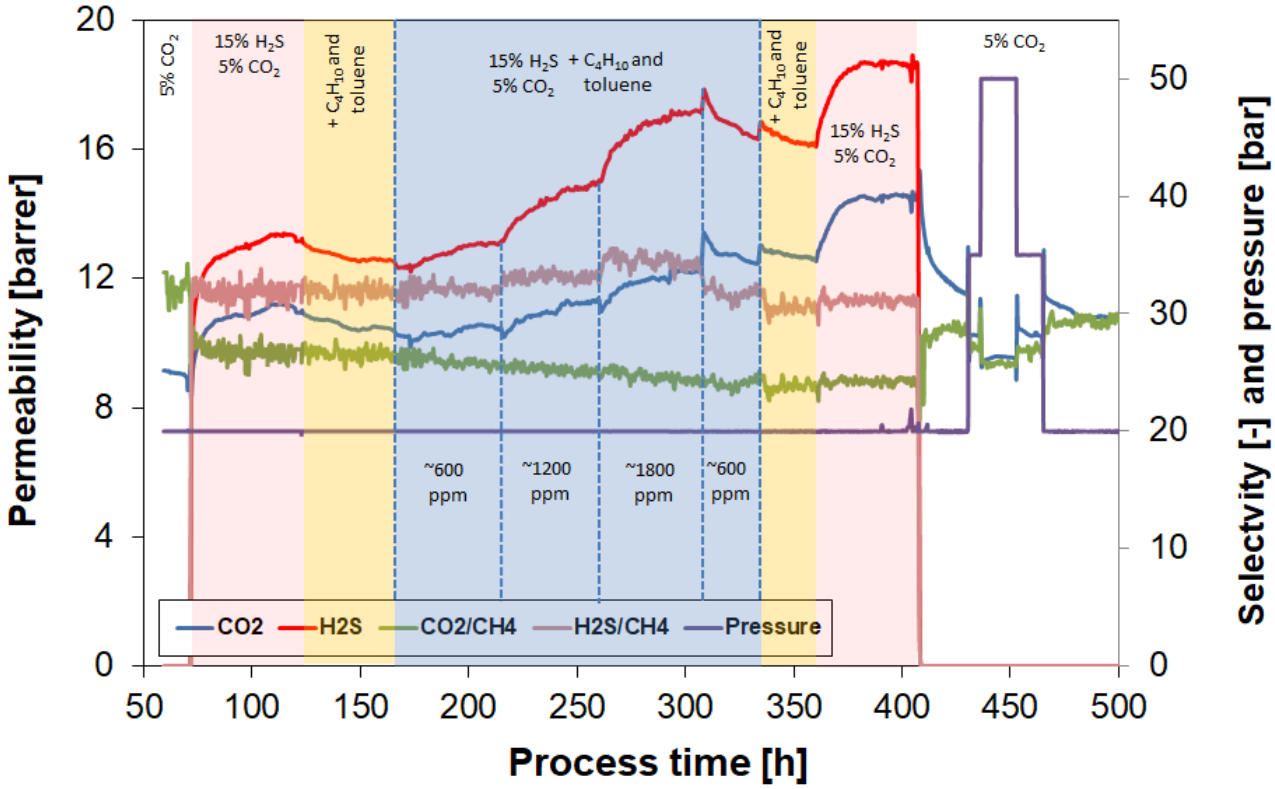

Separation performance of cellulose triacetate dense film membrane in the presence of 15% H_2S containing gas mixtures with various levels of humidity at 20 bar and 30 ° C: After baseline, first 15% H_2S, 5% CO_2 and bal. CH_4 is introduced in the red region, followed by 15% H_2S, 5% CO_2, 3% N-Butane, 300 ppm toluene and bal. CH_4 is switched in the orange region. Subsequently, the 15% H2S and butane/toluene gas mixture with various levels of humidity is present in the blue region. Systematically, the reverse order of gas mixtures trend is also demonstrated for membrane robustness.

Performance and stability of cellulose triacetate membranes in humid high H_2S natural gas feed streams

T.A. Peters[1], L. Ansaloni[1], A. Tena[2,§], O. Karvan[2], T. Visser[2], D. Chinn[3], and N. Bhuwania[3,*]

[1] Department of Sustainable Energy Technology, SINTEF Industry, N-0314, Oslo, Norway

[2] EMI Twente B.V., Postbus 217, 7500 AE Enschede, The Netherlands

[3] Chevron Technical Center, 100 Chevron Way, Richmond, CA, 94802, USA

* Corresponding author: nbhuwania@chevron.com

§ Present address: Surfaces and Porous Materials (SMAP), Institute of Sustainable Processes (ISP), Dr. Mergelina S/n, University of Valladolid, Valladolid, 47011 Spain

Abstract

The current study aims to provide a thorough understanding of the separation performance of the cellulose (tri)-acetate (CTA) membrane material in humid high H_2S natural gas feed streams. The systematic study of the gas separation performances of CTA polymers has been carried out in self-standing symmetric films and asymmetric hollow fiber membranes. The separation performance in H_2S-containing mixtures ($CH_4/CO_2/H_2S$, 80/5/15 mol%) were evaluated at 30 and 50 °C at 20, 35 and 50 bar, including higher hydrocarbons (butane and toluene) in the presence of various levels of humidity, up to 4500 ppm or 80% RH, depending on conditions of temperature and pressure. For the first time, the effect of these contaminants and humidity together under sour gas (15% H_2S) has demonstrated the promising stability of CTA membrane separation performance (both H_2S permeability and H_2S /CH_4 selectivity wise) and with the improvement of permeability due to combination of H_2S plasticization and competitive sorption makes this phenomenon even more attractive and worth studying further.

Keywords: Membrane; CTA; natural gas sweetening; H_2S; CO_2; contaminants; performance.

Contents

1 Introduction

The composition of natural gas can vary over a wide compositional range of CH_4, CO_2, H_2S and hydrocarbons. The maximum allowable concentration of H_2S and CO_2 for pipeline specification natural gas in the U.S. is 4 ppm and 2 mol%, respectively [1]. For the removal of these two gases from natural gas, several solvent-based absorption processes such as Diethanolamine (amines), Sulfinol® (amines), Rectisol® (methanol) or Selexol™ (polyethylene glycol), and adsorption-based (carbonate, or carbon molecular sieves) processes have been developed [2].

Compared to conventional absorption processes, membrane-based gas separation is a technology with low capital cost, potentially high energy efficiency, small footprint, modularity, simple operation, and low maintenance, as well as minimal environmental impact [3]. Gas separation membranes have been widely used for CO_2 removal applications and can come with the added benefit of co-removal of H_2S and H_2O as well. In fact, removal of H_2S from natural gas using membranes can have significant benefits for improving the gas purification of a sour natural gas field and membrane technology being modular can be integrated with rest of the gas treatment plants for de-bottlenecking the plants, reduce sulfur load by diverting the H_2S molecules back to the reservoir through reinjection [4-6].

Currently, the only commercial membranes applied for natural gas sweetening are polymeric, of which the majority (>80%) are based on cellulosic based materials [7]. There have been promising studies from various research groups showing the potential of cellulose triacetate (CTA) and polyimide membranes for removal of H_2S from various hydrocarbon mixtures (including methane, ethane, propane and aromatics like toluene) [8-10]. In this paper, we extend that understanding and perform a systematic parametric study of CTA membranes separation performance under high H_2S containing mixed gases along with varying levels of relative humidity/moisture, and various hydrocarbon chains (including aromatics). As moisture and higher hydrocarbons are important constituents of natural gas fields, it becomes vital to understand the impact of contaminants in H_2S environment for fundamental understanding and application of membranes for industry adaptation.

2 Background

Integrally skinned asymmetric cellulose acetate (CA) membranes are the current industrial standard for the removal of CO_2 from natural gas but show relatively modest permeabilities. In addition, they are perceived to suffer selectivity loss under aggressive feed conditions leading to rather modest selectivity values of 20-30 and 10-20, for the gas pairs H_2S/CH_4 and CO_2/CH_4, respectively. Cellulose acetate membranes show a relatively low H_2S permeability of approximately 4.7-10.2 Barrer, depending on temperature (22 – 80 °C) at low H_2S partial pressure (1 bar) [11]. At higher pressures (34.4 and 48.3 bar, T = 35°C, feed $H_2S/CO_2/CH_4$ = 20/20/60), H_2S permeability values of 8.7 and 39.7 Barrer are obtained, with a H_2S/CH_4 selectivity of 29.7 - 27.4, respectively [12]. Under the same conditions, a CO_2 permeability of, respectively, 8.7 and 27.5 Barrer is obtained at a CO_2/CH_4 selectivity of 29.5 - 19.1. The increase in permeability combined with the decrease in CO_2/CH_4 selectivity with pressure is, generally, related to plasticization phenomena.

In an early work reported by Allied-Signal, the effect of typical natural gas impurities such as H_2O, H_2S, carbonyl sulphide (COS), and hydrocarbons was presented at a feed pressure of around 13.8 bar [13]. In their Exxon field tests, spiral wound cellulose acetate modules did not show any sign of chemical or physical degradation in the natural gas feed containing 17% of H_2S and 44.9% of CO_2, saturated with water. CO_2/CH_4 and H_2S/CH_4 selectivity were in the range of 13-15 and 17-22, respectively. The effect of moisture was separately investigated in a lab environment. For relative humidity of 10% or less, there is no appreciable effect on the carbon dioxide flux. For relative humidity in the range 18-23%, the flux decreased 30% compared to the dry gas flux but recovered when the feed was switched back to dry gas. For relative humidity of 30% and higher, the flux decline was found to be large, rapid and irreversible. In the same work, the effects of water vapor plus hydrogen sulfide are reported. Hydrogen sulfide has a negligible effect on membrane performance if the feed gas is dry. If both hydrogen sulfide and water vapor are present, however, the transmembrane flux is substantially reduced. Li et al. concluded that the processing of streams containing both high concentrations of hydrogen sulfide and water vapor must be avoided with cellulose acetate membranes [13]. Experimental conditions, such as temperature and pressure, however, are not easily extracted from the Allied-Signal report.

A recent study verified the performance of a cellulose tri-acetate hollow fiber membrane in realistic raw natural gas sweetening conditions [8]. In that study, the CTA hollow fiber membrane samples were specially prepared and provided by SLB. A gas composition with high H_2S content (20 mol.%), low CO_2 content (5 mol.%), and significant amounts of C_2H_6 (3 mol.%) and C_3H_8 (3 mol.%) as well as trace amount of toluene (100–300 ppm) with CH_4 comprising the rest of the feed was applied. Various temperatures (35 °C and 50 °C) and pressures (6.9 - 31.3 bar) were considered. On the benefit of controlled plasticization for the CTA hollow fiber membrane, an attractive CO_2 and H_2S permeance (>110 GPU) and selectivity for CO_2 and H_2S over CH_4 (22 and 28, respectively) at 35 °C and 31.3 bar were obtained. Another study applied a H_2S containing gas mixture containing of 5% CO_2, 21% H_2S, 15% C_2H_6, 10% C_3H_8 balanced with CH_4 while mixed-gas permeation tests were carried out at three temperatures, 15 °C, 25 °C, and 35 °C, and four pressures, 15 bar, 29 bar, 39 bar, and 46 bar [10]. It was found that the H_2S mixed-gas permeation increased with increasing feed pressure. At the lower feed pressure between 15 bar and 30 bar, the H_2S/HCs selectivity were essentially stable. However, the selectivity is drastically decreased at the feed pressure of 30 bar and higher. The high condensability and solubility of H_2S at pressures higher than 30 bar would increase the mobility of the CTA polymer chain segments dramatically [10].

Natural gas sweetening by membranes can be challenged by co-existence of condensable hydrocarbons, *e.g.*, C_3+ and toluene, which can compete with H_2S, CO_2 and CH_4 in the sorption in the polymer matrix, therefore hindering the permeation of other components. This was shown by a recent study on cellulose triacetate (CTA) hollow fiber membranes [8]. By increasing the toluene concentration from 100 ppm to 300 ppm, significant reductions in permeance and selectivity were observed for both H_2S/CH_4 and CO_2/CH_4 separations. Moreover, the membrane's stability under aggressive conditions, *e.g.,* high concentration of condensable H_2S, CO_2 as well as various hydrocarbons, high operating pressure ($\gg$ 30 bar), and variation of operating temperature, is also important for future applications. No information of such stability for CTA membranes in the co-existence of both humidity and condensable hydrocarbons is available in literature. Therefore, in this study, we have conducted further evaluations on the performance of cellulose acetate (CTA). The characterization of the separation performances has been performed for sour feed gas including higher hydrocarbons and in the presence of various levels of humidity. To our

148 understanding such evaluation in humid harsh sour conditions, and in the presence of higher
149 hydrocarbons, is not available in current literature.

150 The current study aims thus to provide a thorough understanding of the separation
151 performance of the cellulose (tri)-acetate (CTA) membrane material. Initially, dense-film CTA
152 membranes have been prepared by EMI and sent to SINTEF for thorough characterization with
153 H_2S-containing mixtures. Measurements have initially been performed in a non-H_2S-
154 containing CH_4/CO_2 mixture (5% CO_2 in CH_4) to be able to compare the performance with
155 literature [14-16], and also the membrane stability, before and after H_2S exposure.
156 Subsequently, the separation performance in H_2S-containing mixtures ($CH_4/CO_2/H_2S$, 80/5/15
157 mol%) was thoroughly evaluated at 30 and 50 °C at 20, 35 and 50 bar, including various levels
158 of humidity and in the presence of higher hydrocarbons, such as toluene. In addition, CTA
159 hollow fibers were spun using the dry jet-wet quench technique and evaluated in the same
160 gas mixtures.

161

3 Experimental

3.1 Membrane samples

3.1.1 Self-supported membranes

Cellulose (tri)-acetate (CTA) membrane samples were obtained from EMI Twente. Samples were made using CTA (degree of substitution (DS) ~2.7) from Eastman (CA-398-100) and dichloromethane (DCM) as solvent during casting [15]. The thicknesses of the samples investigated range from approximately 40-60 µm, as detailed in Table 2.

3.1.2 CTA fiber samples

CTA hollow fibers were spun using the dry jet-wet quench technique which is based on non-solvent induced phase separation method. In this technique, a polymer solution in an aprotic solvent is co-extruded with a bore fluid through holes in a spinneret. The spinneret consists of two co-centric nozzles and bore fluid is fed to the inner one while the spinning dope is flowing through the slit between the nozzles. The spinning dope may contain a co-solvent and other additives. The bore solution most of the time is a mixture of the solvent of the spinning dope and at least one non-solvent. The ratio of the solvent and non-solvent(s) depends on the spinning dope and its precipitation behavior. More information on the fundamentals of hollow fiber formation by the non-solvent induced phase separation method is available in the literature [17-20]. N-methyl-2-pyrrolidone (NMP, 99% extra pure) was used as the solvent and received from Themo Scientific. Acetone is used as the co-solvent (Sigma-Aldrich, ≥99.5 ACS reagent). LiCl was introduced to the recipe as non-solvent. It also acts as pore-former (99% by Sigma-Aldrich). Demi water is used as non-solvent in the quench and rinsing baths. LiCl was first dissolved in the NMP/Acetone mixture prior to adding the polymer, which was previously dried in a vacuum oven at 105 °C overnight. The jar was placed on a roller bench and slightly heated using an IR heating lamp. Prior to spinning, the dope was filtered through 25-40 µm metal mesh filter applying 6 bar of N_2-pressure. The filtered dope was directly filled into the container of the spinning system and degassed for at least 24 hours at 50 °C. Table 1 shows the dope compositions and the spinning conditions. The dope and coagulation bath temperatures were fixed at 50 °C for all experiments and one type of spinneret was used (ID Needle of 0.22 mm and OD orifice of 0.61 mm). The other spinning parameters (draw ratio, dope and bore flowrates, N_2 flowrate within the chimney) were altered to achieve a steady spinning session that could yield concentric round hollow fibers with asymmetric morphology with open substructure and outer diameter below 400 µm.

Table 1 *Overview of dope compositions and conditions of spin trials with adjusted recipe.*

	C-CTA-11-2	C-CTA-11-2R
%wt. Polymer	22	22
%wt. NMP	61	61
%wt. Acetone	15	15
% LiCl	2	2
Bore Fluid %wt. (NMP/H_2O)	20/80	20/80
Chimney length (cm)	13	13
N_2-flow chimney (L/min)	2.5	2.5
Dope flow (ml/min)	3.3	3.3
Bore flow (ml/min)	0.56	0.56
Pulling speed (m/min)	9.6	9.6

For all trials, the spun fibers were kept in the post-processing rinsing bath for 2 days before performing the solvent exchange procedure. The post-processing rinsing bath is fed with fresh water continuously. The solvent exchange was performed in 4 steps; in the first two steps, fibers were soaked in methanol for 1 hour each time and for the last two steps were performed in n-Hexane for 1 hour each time. Subsequently, the fibers were air dried and characterized. The spinning session C-CTA-11-22R was performed as the repetition of the session C-CTA-11-2 to check the repeatability and obtain more fibers to build modules for gas permeation measurements. After the preparation of modules with multiple fibers, a polydimethylsiloxane (PDMS) coating was applied on the fibers to seal the possible defects. The elastomer base (SYLGARD 184, Dow Chemicals) and the curing agent were dissolved in n-Hexane and mixed at room temperature for 1 hour. This solution was then diluted to the concentration targeted for the coating. A 2%wt. solution was used for the module with fibers from C-CTA-11-2 and a 1% solution was used for the modules with fibers from C-CTA-11-2R. The solutions were filled into the modules and drained after 10 seconds. After air drying for 4 hours, the PDMS was further crosslinked in a convection oven at 45 °C overnight. Modules were pre-tested to verify the absence of defects and then shipped to SINTEF for further permeation tests.

3.2 Gas permeation properties

For the testing of the self-supported CTA samples, a high-pressure Millipore 47 mm HP Holder (active area 9.6 cm^2) was applied. Connections for feed, retentate, sweep and permeate streams were installed with the help of Swagelok® connectors. The Millipore module is shown in Figure 1. Circular CTA samples for the permeation were easily punched out from the free-standing CTA film and applied in the module. In between the porous filter plate and the CTA film a porous 25 µm-thick polypropylene (PP) film (Celgard® 2500) to prevent that the CTA film was mechanically damaged during the high-pressure operation. Without the Celgard® film it was observed that the CTA membrane was mechanically deformed (around 5 µm) from polymer extrusion into the openings of the Millipore back-pressure support screen.

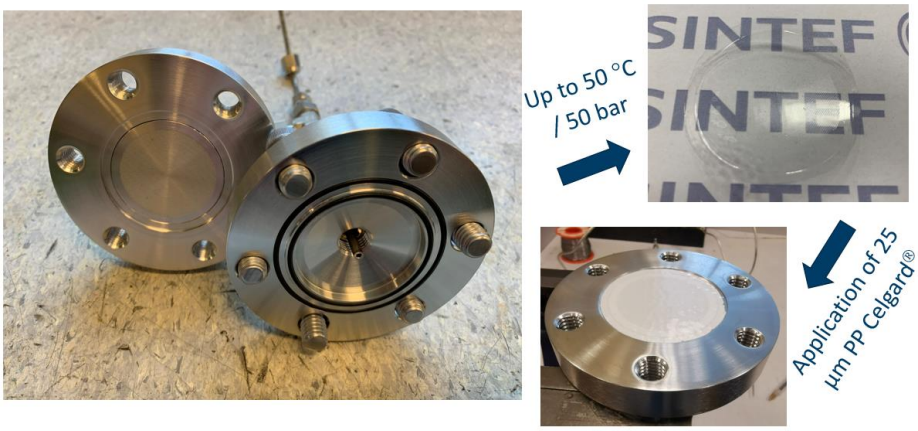

Figure 1 Millipore 47 mm HP membrane holder and integration of the CTA film. The CTA film is supported by a porous 25 µm-thick polypropylene (PP) film (Celgard®).

All gas permeation measurements were conducted using the constant-pressure method, analogue to ASTM D3985 – 17, through employing gas chromatography (GC) analysis on the permeate stream, in a permeation set-up under mixed gas conditions. The setup was designed to withstand a pressure up to 92 bars, and the membrane module was placed in a Memmert UF450 forced air circulation oven for temperature control. Automated mass flow controllers (MFC) (Bronkhorst High-Tech B.V.) were used to control the gas supply to the feed and permeate side of the membrane module. A controlled evaporation mixing (CEM) system was installed for the accurate introduction of low levels of humidity (Bronkhorst High-Tech, CEM W-101A-C10-K, size 2 – 100 µg/h). The pressure of the feed side was controlled with the help of a back-pressure controller (Bronkhorst High-Tech, P-512C equipped with F-033C control valve, max. 92 bar). At the permeate side, argon was applied as a sweep flow gas. The permeate side was at atmospheric pressure, and the permeate flow was measured using an

automated mass flow meter (Bronkhorst High-Tech, F-101D, size 100 mL/min). A micro-GC (Agilent 490) equipped with a thermal conductivity detector (TCD) was employed to monitor the permeate composition. The micro-GC was calibrated for low concentrations of CO_2 (0-12 vol.%), CH_4 (0-5 vol.%) and H_2S (0-25 vol.%)) in Argon using $CO_2/CH_4/H_2S$ mixtures prepared in the lab using calibrated flow controllers. A good linear fit (R^2 = ≥0.999) was obtained for the GC response as a function of CO_2, H_2S, and CH_4 content. The flux of the respective gaseous components was calculated from the measured absolute permeate flow and the permeate composition measured by the GC. Permeability values were expressed at 20 °C and 1.013 bar (1 atm) in units of Barrer. Selectivity is defined as the ratio of permeability of the two gaseous components.

Bottled pre-mixed gas cylinders (Nippon gas) were employed. Investigated gas mixtures include a mixture containing 5% CO_2 in CH_4, a mixture containing 15% H_2S and 5% CO_2 in CH_4, and a mixture containing butane (3%) and a trace amount of toluene (300 ppm) maintaining 15% H_2S, 5% CO_2, in CH_4 Two temperatures, i.e., 30 °C and 50 °C, and three pressures, ranging from 20 bar to 50 bar, were considered in the study. Table 2 provides an overview of the varying test conditions for the investigated self-standing CTA samples.

Table 2 Self-supported CTA membrane samples and conditions investigated.

Sample	Thickness [µm]	5% CO_2	Humid 5% CO_2	15% H_2S	Humid 15% H_2S	C_4/toluene	Humid C_4/toluene
CTA#2		x					
CTA#3		x		x			
CTA#5	44.9 ± 5.1	x	x				
CTA#6	46.3 ± 2.8	x		x	x		
CTA#7	45.6 ± 5.6	x		x	x		
CTA#9	63.1 ± 7.3	x		x		x	
CTA#10	34.9 ± 1.5	x		x		x	x

4 Results and discussion

4.1 Self-standing CTA samples

4.1.1 Permeation in CO_2/CH_4 including humidity

The performance of the individual CTA membrane films was initially evaluated up to 50 °C and 50 bar in a pre-mixed feed consisting of 5% CO_2 in CH_4. In total, seven samples were evaluated for their performance. The obtained membrane performance with standard deviation can be seen in Figure 2, while the numerical values for obtained permeability and selectivity are given in Table 3.

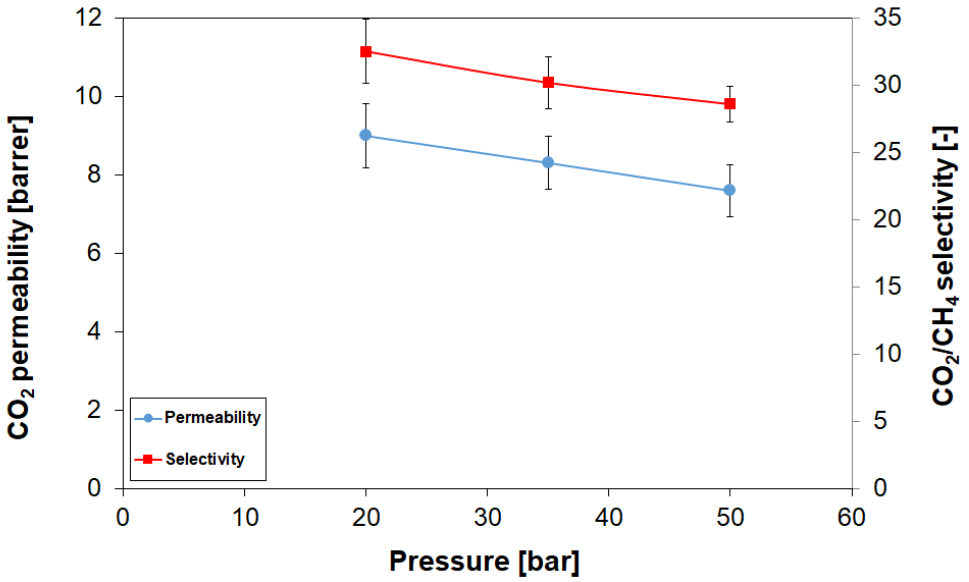

Figure 2 Initial performance of CTA samples as function of pressure at 30 °C

Table 3 Numerical values for obtained permeability and selectivity, 30 °C, 5% CO_2 in CH_4 as feed.

Temperature [°C]	Pressure [bar]	CO_2 permeability [Barrer]	CH_4 permeability [Barrer]	CO_2/CH_4 selectivity [-]
30	50	7.6 ± 0.7	0.27 ± 0.03	28.6 ± 1.3
30	35	8.3 ± 0.7	0.28 ± 0.04	30.2 ± 1.9
30	20	9.0 ± 0.8	0.28 ± 0.04	32.5 ± 2.4

The obtained CO_2 permeability and CO_2/CH_4 selectivity is 9.0 Barrer and 32, respectively at 20 bar. For CTA self-standing films with similar thickness, Scholes et al. report ~7-8 Barrer [14]. The obtained permeability and selectivity also agree well with data reported by Swaiden et al. [16]. It can thus be concluded that the samples result in reproducible performance. The effect of humidity in 5% CO_2 in CH_4 as feed was subsequently investigated. Figure 3 shows the effect

of humidity on the CO_2 permeability and CO_2/CH_4 selectivity at a pressure of 20, 30 and 35 bar. At each humidity level the performance was left to stabilize for at least 12 hours.

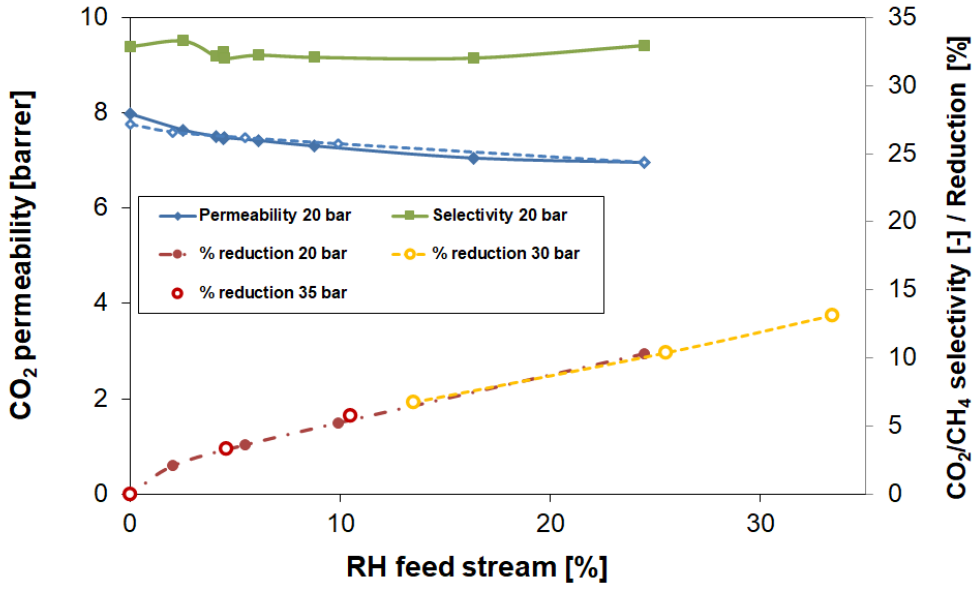

Figure 3 *Effect of relative humidity on CTA performance, 30 °C and varying pressure. Sample CTA#5.*

At 20 bar and relatively short-term exposure to relative humidity levels of 2.5 – 25% RH (50 – 500 ppm), the CO_2 permeability is reduced by around 10 – 13%, at unchanged CO_2/CH_4 selectivity. At these humidity levels, the reduction seems reversible. This behavior agrees with the data from Li et al. [13] that show no significant effect on the CO_2 flux at relative humidity levels of 10% or less. For relative humidity in the range 18-23%, the flux decreased 30% compared to the dry gas flux, but recovered when the feed was switched back to dry gas. For relative humidity ≥ 30%, the flux decline was found to be large, rapid, and irreversible. Subsequently, the humidity was investigated at slightly more elevated pressures, i.e., 30 and 35 bar. The results are plotted as function of the relative humidity of the feed in Figure 3 showing that the percentage reduction in CO_2 permeability follows a relation with the relative humidity of the gaseous feed, at least within the conditions investigated.

4.1.2 Permeation in ternary mixtures including 15% H_2S and humidity

Subsequently, the CTA performance has been investigated in a sour feed gas containing 15% H_2S. Membrane CTA#3 was followed over time while varying pressure at both 30 and 50 °C in the presence of 15% H_2S. The sample was tested for an overall period of 1000 hours, of which approximately 480 hours was in the presence of 15% H_2S. As an example, the time-dependent flux and selectivity behaviour at 30 °C, at pressures of respectively 20, 35 and 50 bar is given in Figure 4.

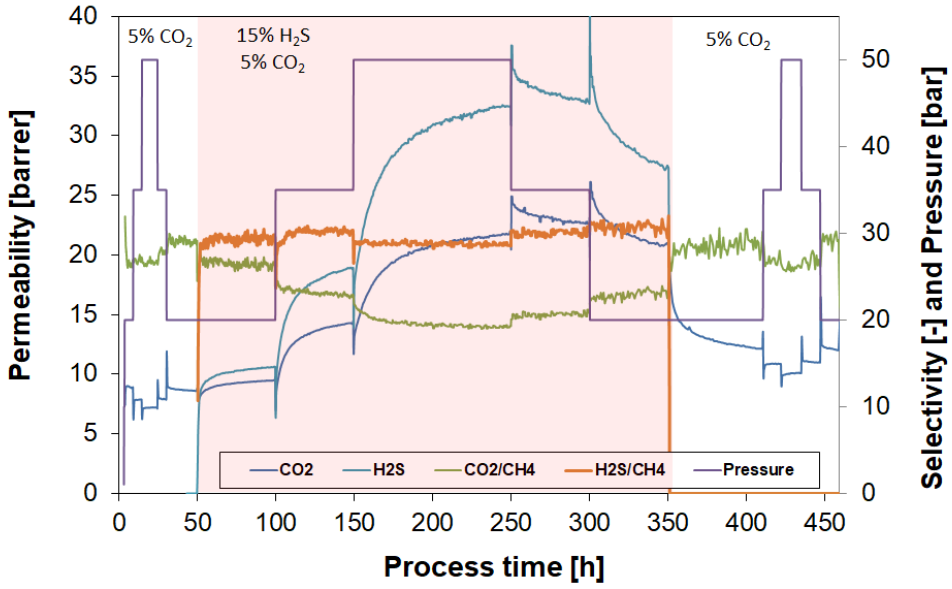

Figure 4 Time-dependent performance of sample CTA#3 in the presence of 15% H_2S at 30 °C. H_2S is present in the red region.

Compared to the baseline performance in 5% CO_2 in CH_4, the introduction of H_2S results at 20 bar (see Figure 4 at process time between 50 and 100h) in a gradually increasing trend of both the CO_2 and H_2S permeability over time, combined with a slight decrease in CO_2/CH_4 selectivity. This effect is magnified at the higher pressures (after 100 and 150h the pressure was increased to respectively 30 and 50 bar). For example, the CO_2 and H_2S permeability increases respectively by approximately 30 and 40% over a period of 100 hours at 50 bar. This might be explained by a gradually controlled plasticization induced by H_2S. The slow kinetics can be explained by the fact that a relatively thick self-supported membrane sample is applied for the current tests. Compared to the permeability prior to any H_2S exposure, the H_2S introduction results in a large increase in CO_2 permeability (10-200% for 20 – 50 bar) at the expense of a minor drop in CO_2/CH_4 selectivity (9-27%). Figure 5 shows the gas separation performance in the presence of 15% H_2S as function of pressure (full lines: incremental pressure; dotted lines: decremental pressure). The increased permeability is rather long-lasting for these thick self-supported samples. The total sour gas selectivity, $(CO_2+H_2S)/CH_4$, shows values around 54-48, while the total sour gas permeability equals 48 (20 bar) – 54 (50 bar) Barrer. The removal of H_2S from the feed leads to a much faster decrease in permeability (see process time between 350 and 400 hours in Figure 4), while the CO_2/CH_4 recovers quickly back to the CO_2/CH_4 selectivity prior to any H_2S exposure. However, even after 100h of sweet operation, the permeability lies 40% above its initial value prior to any H_2S exposure.

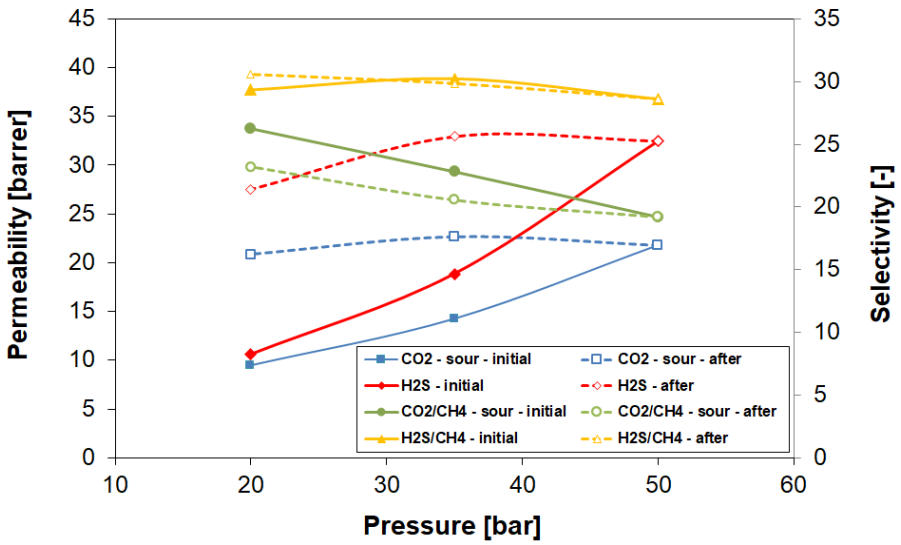

Figure 5 Performance of CTA#3 in the presence of 15% H_2S as function of pressure during the increase in pressure (full lines) and decrease in pressure (dotted lines), T = 30 °C.

These results agree rather well with expectations from existing literature. Cellulose acetate membranes show a relatively low H_2S permeability of approximately 4.7-10.2 Barrer, depending on temperature (22 – 80 °C) at low H_2S partial pressure (1 bar) [11]. However, at higher pressure (T = 35°C, feed $H_2S/CO_2/CH_4$ = 20/20/60), a H_2S permeability of 8.7 and 39.7 Barrer is obtained at 34.4 and 48.3 bar respectively, with a H_2S/CH_4 selectivity varying between 29.7 and 27.4 [12]. Under the same conditions, a CO_2 permeability of respectively 8.7 and 27.5 Barrer is obtained with a CO_2/CH_4 selectivity of 29.5 - 19.1. The increase in permeability combined with the decrease in CO_2/CH_4 selectivity with pressure might be related to plasticization phenomena expected due to the high condensability of H_2S and CO_2, which leads to high solubility in the polymer matrix, increasing the mobility of the polymer chain segments, thereby increasing gas permeation [8]. As expected also, CO_2/CH_4 selectivity decreases gradually as plasticization occurs. However, the plasticized CTA membrane shows an unexpectedly stable H_2S/CH_4 selectivity. A similar behavior has been reported for CTA hollow fiber membranes [8] and glassy polyimide-based dense film membranes for $H_2S/CO_2/CH_4$ ternary mixture separation [9], illustrating the controlled plasticization benefits of H_2S.

Subsequently, the performance of the CTA membranes has been investigated in humid sour feed gas streams containing 15% of H_2S. Figure 6 shows the time-dependent performance in the presence of 15% H_2S at 30 °C during humidity exposure up to 90% RH at 20 bar (CTA#7) and 50 bar (CTA#6), respectively. Initially, the performance is left to stabilize in the sour feed gas (5% CO_2, 15% H_2S in CH_4) for around 4 days. This establishes a proper baseline prior to the

humidity introduction. Then, the performance in humid 15% H_2S is investigated at varying water vapor content over a period of around 200 hours. Finally, the performance in the dry sour feed gas (5% CO_2, 15% H_2S in CH_4) is again verified to investigate any hysteresis effects.

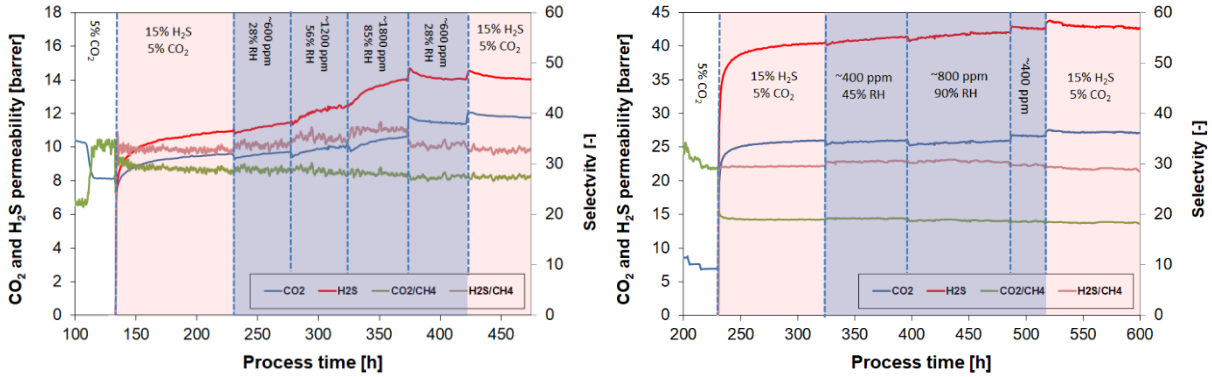

Figure 6 Time-dependent performance of CTA in the presence of 15% H_2S at 30°C, (a) 20 bar, sample CTA#7;(b) 50 bar, sample CTA#6. Humidity is added in the blue region. H_2S is present in the red region.

At 20 bar (Figure 6a, 130h) the introduction of H_2S results in a minor gradually increasing behavior of both the CO_2 and H_2S permeability over time, combined with a decrease in CO_2/CH_4 selectivity. Compared to the permeability prior to any H_2S exposure, the H_2S introduction results in an increase in CO_2 permeability from 8.1 to 9.6 Barrer at the expense of a reduced CO_2/CH_4 selectivity from 33.6 to 28.6 under the current conditions (30 °C and 20 bar). The H_2S permeability equals 10.9 Barrer. Thereafter (Figure 6a, 230h) humidity is introduced at a water content of 600 ppm (28% RH). This results in a slow gradual increasing behavior in both CO_2 and H_2S permeability. During the next 2 days of operation at 600 ppm the CO_2 and H_2S permeability increased from respectively 9.4 and 10.9 Barrer to 9.7 and 11.5 Barrer. The permeability increase occurs at seemingly unchanged CO_2/CH_4 and H_2S/CH_4 selectivity. The further increase in humidity, first to 1200 and then to 1800 ppm results in a similar effect. Upon changing the humidity level initially both the CO_2 and H_2S permeability show some flow stabilization, after which followed a slow and gradually increasing permeability behavior. Our hypothesis is in the higher H_2S environment, the combination of H_2S plasticizing and hydrophilic nature of CTA is enabling the swelling of polymer chains which allows the H_2S molecules to pass through, but the there is still significant competitive sorption between condensable gases (H_2S, CO_2 and H_2O) vs. CH_4 which helps in preserving or slightly increasing selectivity. H_2S separation behavior seems to benefit from the presence of high moisture content. The reduction in humidity from 1800 to 600 ppm (Figure 6a, 375 h) does not trigger an immediate decrease in permeability, indicating there is probably some

hysteresis at higher humidity content. Considering the thickness and density of the samples, it will take additional time for the polymer chain to return to the original state. Comparing initial and post-humid membrane performance shows that the humidity exposure has increased the CO_2 and H_2S permeability from respectively 9.6 and 10.9 Barrer to 11.8 and 14.2 Barrer, even after 2 days of operation in dry gas. The H_2S/CH_4 selectivity is not affected by the humid operation, while the CO_2/CH_4 selectivity obtained after the humid operation is somewhat lower compared to the initial value, i.e., 27.0 compared to 28.6. At 50 bar a similar behavior is observed though the plasticization upon H_2S introduction at 50 bar is much larger, explained by the higher partial pressure of H_2S in contact with the membrane as previously explained in Figure 5. The H_2S introduction at 50 bar results in a large increase in CO_2 permeability from 6.9 to 26.0 Barrer (9.6 Barrer at 20 bar) at the expense of a reduced CO_2/CH_4 selectivity from 29.2 to 19.0. The H_2S permeability after 100 h of stabilisation equals 40.5 Barrer (10.9 Barrer at 20 bar). Then humidity is introduced at a level of 400 ppm (Figure 6b, 320h, 45% RH). Similar to what was observed at 20 bar, this results in a minor immediate decrease in CO_2 permeability, which is followed by a gradual increasing trend observed especially for the H_2S permeability. During 3 days of operation, the CO_2 and H_2S permeability increases from respectively 25.4 and 40.2 Barrer to 26.0 and 41.3 Barrer. The humidity introduction also triggers a minor increase in the H_2S/CH_4 selectivity at unchanged CO_2/CH_4 selectivity. The subsequent further increase in humidity to 800 ppm generates in a similar response on the permeability. Compared to the observations at 20 bar (Figure 6a), the various humidity levels affect the membrane performance to a minor effect at 50 bar, both in absolute and relative amount. It seems that the additional swelling and/or plasticization effect of humidity at 50 bar is little compared to the already highly plasticized/swollen membrane at 50 bar 15% H_2S. Moreover, the higher partial pressure of each gaseous component results in a stronger competition to water molecules to solubilize within the polymeric matrix, possibly limiting the water uptake. The reduction in humidity at 50 bar from 800 to 400 ppm (Figure 6b, 480h) and subsequently complete removal of humidity (Figure 6b, 515h) results in the opposite behaviour. An initial minor decrease in permeability is followed by a gradually decreasing trend. It should be noted that from the moment the humidity was decreased (~475 hours), both the CO_2/CH_4 and H_2S/CH_4 selectivity seemingly started to decline. The exact reason for this is unclear, but it may be related to the drying of acidic droplets on the membrane surface possibly formed during the high humidity conditions (800 ppm ≈ 95% RH).

4.1.3 Effect of higher hydrocarbons including 15% H_2S and humidity

Subsequently, measurements were performed in the presence of higher hydrocarbons (3% butane and 300 ppm toluene) in the presence of humidity. For this investigation, new membrane samples were applied to provide a valid comparison of membrane performance under different test conditions.

Figure 7 shows the time-dependent performance in the presence of 15% H_2S at 30 °C and subsequently 20, 30 bar (from 210 h) and 20 bar (from 475 h). Butane and toluene presence is indicated by the orange region. Prior to the introduction of butane and toluene, the membrane performance was left to stabilize in the feed mixture containing 15% H_2S. The observed trend upon H_2S introduction agree well with those previously observed in both Figure 4 and Figure 6a.

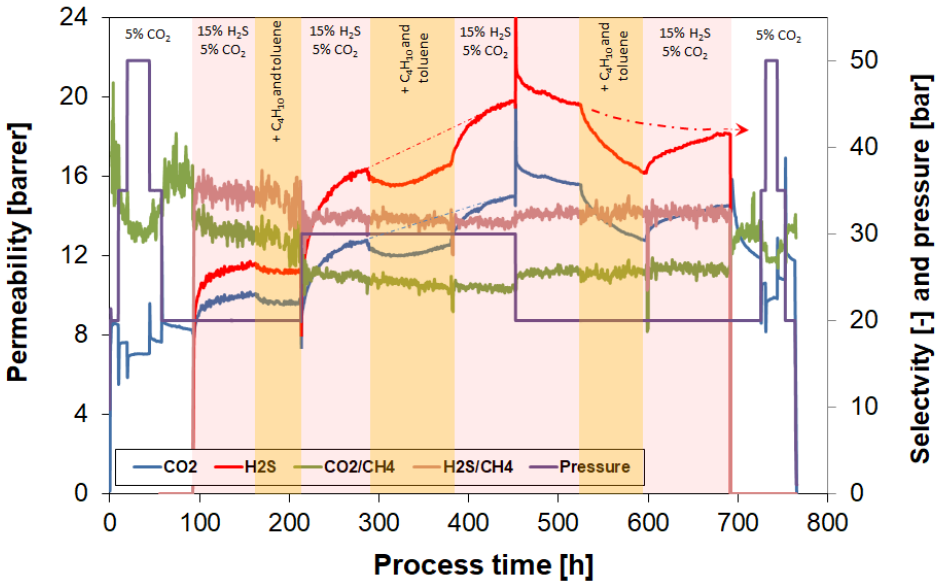

Figure 7 Time-dependent performance of sample CTA#9 in the presence of 15% H_2S at 30 °C and subsequently 20 and 30 bar (from 210h). Butane and toluene are added in the orange region. H_2S is present in the red region.

After a stabilization period of around 50 h in 15% H_2S mixture (5% CO_2 and rest CH_4), a new gas mixture of 15% H_2S + 5% CO_2 + 3% butane, 300 ppm toluene and bal. CH_4 was introduced to the membrane (Figure 7, 160 h) to evaluate the individual effect of C_4/toluene on the CTA performance. This introduction results in a minor inhibition of both the CO_2 and H_2S permeability. After 2 days of exposure, both the CO_2 and H_2S permeability have decreased by around 4%. Both the CO_2/CH_4 and H_2S/CH_4 selectivity are seemingly unaffected at these operating conditions (30 °C and 20 bar). After removal of butane and toluene the pressure was increased to 30 bar, which, as expected, resulted in higher values of both the CO_2 and H_2S

permeability at the expense of slightly reduced values of both CO_2/CH_4 and H_2S/CH_4 selectivity. After a stabilization period of around 72 h, butane and toluene were subsequently introduced, which again resulted in a gradual inhibition of both the CO_2 and H_2S permeabilities at otherwise unchanged CO_2/CH_4 and H_2S/CH_4 selectivities. Comparing the obtained permeability with the extrapolated CO_2 and H_2S permeabilities (dotted line in Figure 7) the magnitude of inhibition is around 10% (30 °C and 30 bar). Note that the gradual decline in permeability is shifted to a gradual increase after around 330 h. At this point, the flux-increasing effect of H_2S plasticization at 30 bar prevails over the flux behavior. The removal of butane and toluene from the feed stream results in the recovery of the flux, seemingly close to the extrapolated performance in the absence of these higher hydrocarbons. Subsequently, the effect of butane and toluene was investigated for a second time at 20 bar. For this, the membrane was again first left to stabilize at 20 bar in a feed mixture of $CH_4/CO_2/H_2S$, 80/5/15. After approximately 3 days, butane and toluene were added to the feed mixture for a period of 3 days (Figure 7, 520 h). Again, the introduction of butane and toluene results in an inhibition of both the CO_2 and H_2S permeability, though compared to the initial exposure to the hydrocarbons at 20 bar, the flux inhibition is larger; ~17% compared to the initial 4%. Both the CO_2/CH_4 and H_2S/CH_4 selectivities are seemingly unaffected at these operating conditions (30 °C and 20 bar). The removal of butane and toluene from the feed stream (process time 600 h) results in a flux recovery, potentially close to the extrapolated performance in the absence of these higher hydrocarbons. In general, highly condensable gases with large kinetic size, such as toluene, compete with H_2S and CO_2 by sorption but can also hinder their diffusion [8]. Therefore, at limited absolute pressure, a higher toluene partial pressure results in decreased H_2S/CH_4 and CO_2/CH_4 selectivities. Nevertheless, the controlled plasticization of the CTA membrane at elevated H_2S partial pressure creates additional free volume (sorption-favored) and increased mobility (diffusion-favored) for all gas molecules. Potentially, the enhanced detrimental effect of toluene on the CTA performance at elevated pressure is offset by the new “opportunities” for permeation [8].

In the following, the CTA performance has been investigated in sour feed gas streams containing 15% of H_2S including higher hydrocarbons (3% butane and 300 ppm toluene) at humidity at levels between 600 – 1800 ppm (20 bar, 30 °C; RH = 28-85%). No information on the performance of CTA membranes in the co-existence of both humidity and condensable

hydrocarbons is available in literature. The results are presented in Figure 8 during which the membrane (CTA#10) was operated in humid 15% H_2S including higher hydrocarbons from a process time of 170 h. Initially, 15% H_2S (with no high hydrocarbons or moisture) was introduced at 70 hours, and then switched to 15% H_2S + C4/toluene mixture at 125 hours. Even though a similar behaviour was observed compared to sample CTA#9, the CO_2 (11.2 versus 10 Barrer) and H_2S (13.4 versus 11.6 Barrer) permeabilities in the presence of 15% H_2S were slightly higher. This can be explained by the lower thickness of CTA#10 leading to a potentially larger effect of plasticization. The introduction of butane and toluene (without humidity) reduced the permeability by around 8%. This reduction is also larger compared to the CTA#9 sample, for which the reduction was found to be ~4% at 20 bar.

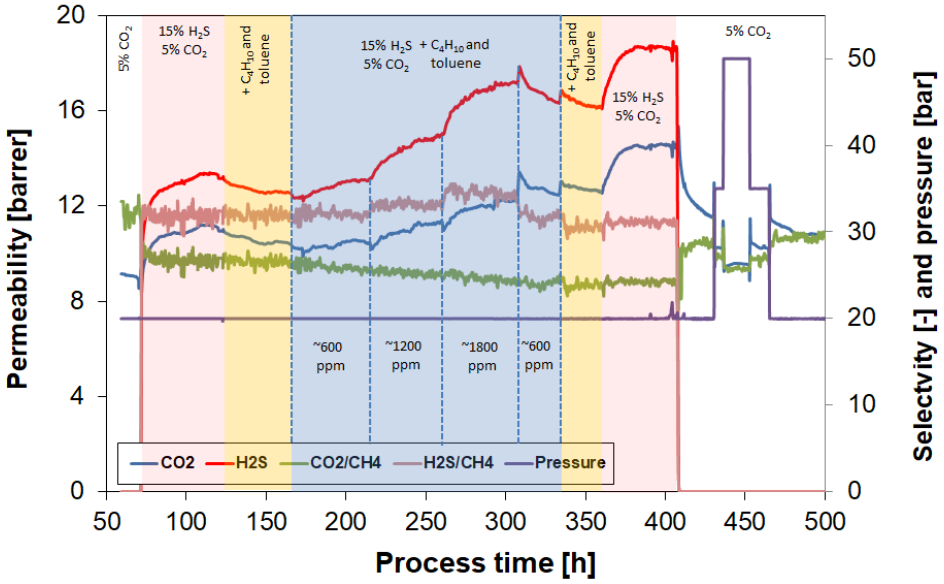

Figure 8 Performance of sample CTA#10 in the presence of 15% H_2S at 30 °C and 20 bar at various levels of humidity. Butane and toluene are added in the orange region. H_2S is present in the red region. Humidity (including H_2S and butane/toluene) is present in the blue region.

Subsequently, humidity is introduced at a level of 600 ppm, which resulted in a slow gradual increasing trend in both the CO_2 and H_2S permeability. During 2 days of humid operation the CO_2 and H_2S permeability increased from 10.2 and 12.3 Barrer to 10.5 and 13.1 Barrer, respectively. This increase occurred at a seemingly unchanged H_2S/CH_4 selectivity, but a decreasing CO_2/CH_4 selectivity trend. The further increase in water content to 1200 ppm and thereafter to 1800 ppm generated a similar response on the permeability; an immediate flow stabilization, followed by a gradually increasing behaviour. Compared to dry operation, the CO_2 and H_2S permeability at 1800 ppm humidity increased from 10.2 and 12.3 Barrer to 12.2 (+19%) and 17.1 (+38%) Barrer, respectively. The larger increase in H_2S permeability resulted

in an increased H_2S/CH_4 selectivity during humid operation. Note, however, the gradual decrease in CO_2/CH_4 selectivity during the humid operation. The reduction in humidity from 1800 to 600 ppm and subsequent complete removal of humidity resulted in the opposite behaviour; an initial minor increase in permeability followed by a gradual decreasing trend. The permeability enhancement takes time to return to its original value after humidity removal. The slow kinetics can be explained by the fact that experiments are performed on a relatively thick self-supported membrane sample. Therefore, in the following, CTA hollow fibers were spun and evaluated in the same gas mixtures, including higher hydrocarbons in the presence of various levels of humidity.

4.2 CTA hollow fiber samples

4.2.1 CTA hollow fiber membrane spinning

Initially, it was targeted to obtain hollow fibers with outer diameter smaller than 400 µm and the wall thickness to be around 100 µm to get a burst pressure over 30 bars (inside out). However, to reach the target, the wall thickness was increased to 150 µm. As a result of this necessity, the fiber outer diameter was set above 644 µm. Besides the burst pressure measurements, fibers were also characterized by single gas permeation measurements and SEM imaging. Hollow fiber modules with 4 connections (feed, retentate, sweep, permeate) tested under 3 bar transmembrane pressure with atmospheric permeate side pressure at 35°C for N_2 and CO_2. The CO_2/N_2 perm-selectivity value was considered as an indication of the formation of a successful defect-free membrane module that could be used for extended permeation tests. Results of characterization studies are given in Table 4. Cross-sectional images of the C-CTA11-2 and C-CTA-11-2R fibers from are shown in Figure 9. Images indicate an open asymmetric substructure with a dense skin layer.

Table 4 Gas permeation properties at 35°C and burst pressure of fibers obtained in the spinning trials.

Batch	CO_2-permeance (GPU)	CO_2/N_2-Selectivity (-)	Dimensions OD/wall (µm)	Burst pressure (bar)
C-CTA-11-2	72*	29*	644 / 186	30-33
C-CTA-11-2R	100-120*	32*	644 / 177	30-33

* After PDMS-coating

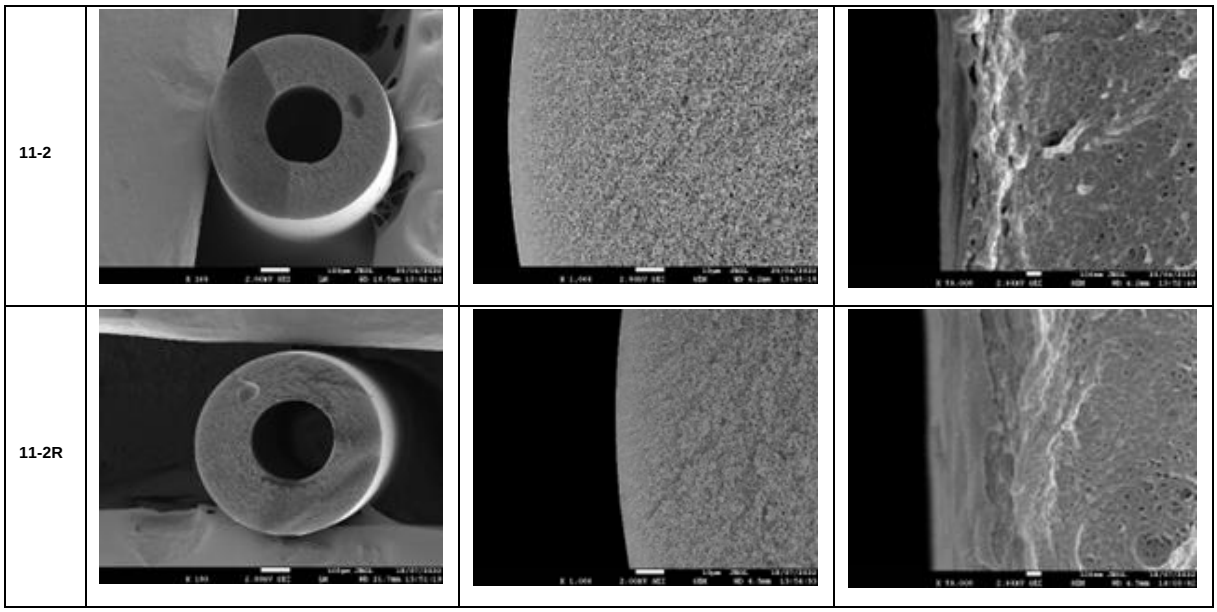

Figure 9 Cross-section of fibers obtained in sessions 11-2 and 11-2R showing overview, wall and outside skin morphology.

4.2.2 CTA fiber module testing in 15% H_2S including humidity

One sample from the C-CTA-11-2R spinning session was used to investigate the CTA fiber performance in the feed mixture containing 15% H_2S including various levels of humidity. For reducing the flow distribution variance and stage cut during experimentation, this module has a relatively short active length and has only two fibers installed, resulting in an active membrane surface area of 5.4 cm^2. Figure 10 shows the time-dependent performance of module C-CTA-11-2R-X. The sample was tested for a total period of 1130 h, exposing the sample for approximately 600 h to 15% H_2S out of which 180 h in presence of humidity. Especially the longer-term performance stability in dry and humid atmosphere was investigated. For the whole test duration, the temperature and pressure were kept at 30 °C and 20 bar, respectively.

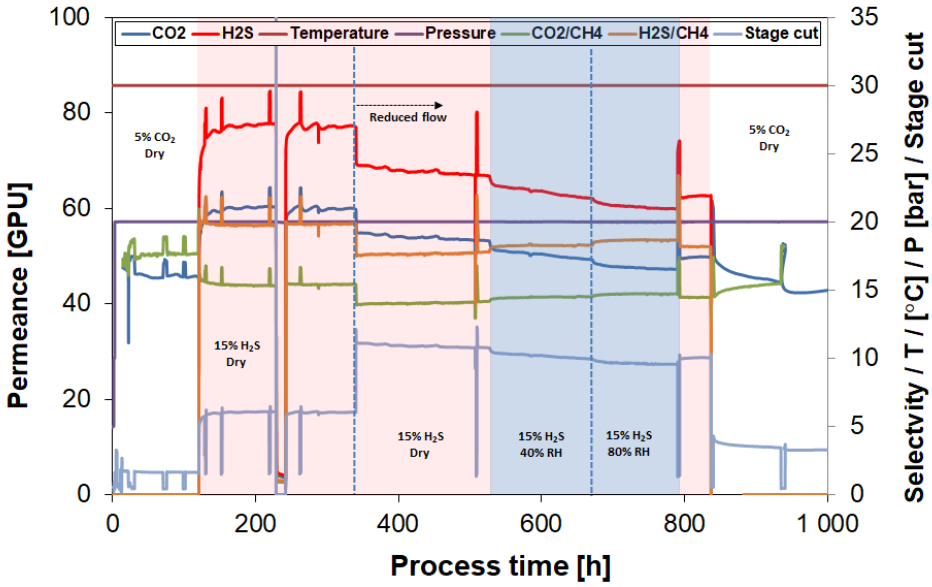

Figure 10 Module C-CTA-11-2R-X, performance as function of time and conditions. H_2S is present in the red region. Humidity (in addition to H_2S) is present in the blue region. T = 30 °C and P = 20 bar. The peaks in the graph are obtained at an increased feed flow rate. Between 230 and 245 h the module was in static gas conditions (no feed flow).

In the initial 5% CO_2 feed, the C-CTA-11-2R-X module shows, respectively, a CO_2 permeance and CO_2/CH_4 selectivity of 54.2 GPU and 18.7, respectively, at stage-cut below 2%. After approximately 120 h, the feed gas was switched to 5% CO_2, 15% H_2S in CH_4. Upon H_2S introduction the CO_2 permeance increased to 65.3 GPU, while the CO_2/CH_4 selectivity was reduced to 15.6. The H_2S permeance stabilized after around 100 h at a value of around 65 GPU at H_2S/CH_4 selectivity of 19.8. The above-mentioned performance data were all obtained at a stage-cut of around 5%. Even though such stage cut is normally low enough to minimize concentration polarization on the upstream membrane side [8], an improved separation performance is obtained by lowering the stage-cut as shown in Figure 11 showing the high flux of the CTA hollow fiber membranes in high H_2S conditions. Numerical values for performance at respectively low and higher feed flow rate are given in Table 5.

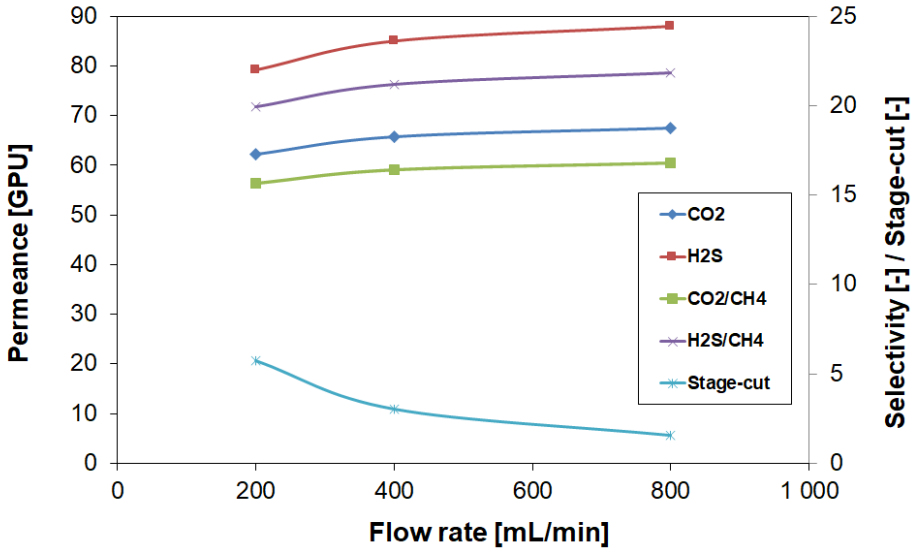

Figure 11 *Module C-CTA-11-2R-X, effect of feed flow rate on performance in 15% H_2S. T = 30 °C and P = 20 bar.*

Table 5 *Module C-CTA-11-2R-X, performance at respectively low/higher feed flow rate, T = 30 °C and P = 20 bar.*

Condition	Flow / stage-cut	T [°C]	P [bar]	CO_2 [GPU]	H_2S [GPU]	CO_2/CH_4	H_2S/CH_4
5% CO_2	Low / 5%	30	20	49.8	-	17.4	-
15% H_2S		30	20	65.3	84.0	15.6	19.8
5% CO_2	High / 1%	30	20	54.2	-	18.7	-
15% H_2S		30	20	69.6	91.3	16.6	21.8

For around 200 h, stable performance was obtained, but a reduction in the feed flow rate applied after around 340 h triggered a decline in both CO_2 and H_2S permeance combined with lower values for both CO_2/CH_4 and H_2S/CH_4 selectivity.

After approximately 525 h, humidity was introduced to the 15% H_2S feed gas. The humid operation during around 265 h in 15% H_2S can be seen in Figure 10. Initially, around 800 ppm of humidity (~40% RH) was introduced. The addition of humidity resulted in a slight increase of both H_2S/CH_4 and CO_2/CH_4 selectivity at a minor decrease in both CO_2 and H_2S permeance. However, the on-going decline in performance that was initiated when lowering the feed flow rate (340 h) seems to be accelerated after the humidity introduction. During the humid operation for around 250 h (40% RH and 80% RH), a 7-8% drop in CO_2 and H_2S permeance was observed. As the CH_4 permeance reduce to a larger extent (~10%), the CO_2/CH_4 and H_2S/CH_4 selectivities increased marginally (2-3%).

To establish that the reduction in H_2S and CO_2 gas permeance (even in presence of humidity) is mainly caused by the high stage cuts, we attempted to run the experiment/gas permeation for a short duration at a large feed flow rate by increasing by a factor of eight, reducing stage-

cut to close to 1% from 790-795 h. The results can be seen in Figure 12 while the numerical values are given in Table 6. Figure 12 starts at low feed flow (stage-cut around 10%) in 80% RH. Then the flow was increased by a factor of 8 (stage cut reduced to ~1.5%). After 2 h in wet conditions, the humidity was removed at unchanged feed conditions. Thereafter, the feed flow rate was again reduced to a stage-cut of around 1.5%.

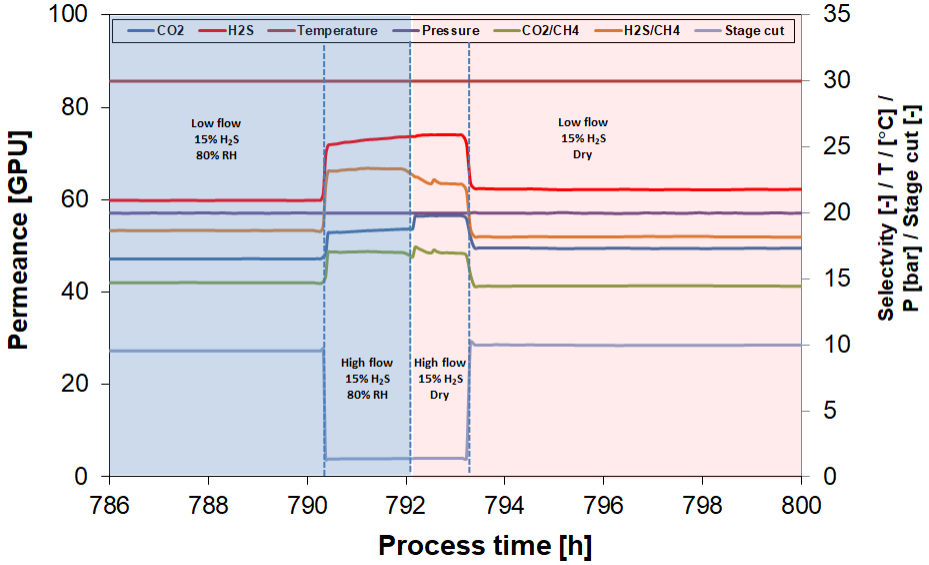

Figure 12 Module C-CTA-11-2R-X, close-up of performance during humidity removal. T = 30 °C and P = 20 bar. H_2S is present in the red region. Humidity (in addition to H_2S) is present in the blue region. The peaks in the graph are obtained at an increased feed flow rate.

Table 6 Module C-CTA-11-2R-X, performance at respectively low/higher feed flow rate in respectively dry and humid conditions, T = 30 °C and P = 20 bar.

Condition	Flow / stage-cut	T [°C]	P [bar]	CO_2 [Barrer]	H_2S [Barrer]	CO_2/CH_4	H_2S/CH_4
Humid 15% H_2S	Low / 10%	30	20	51.4	65.2	14.7	18.7
	High / 1.5%	30	20	58.2	79.8	17.0	23.4
Dry 15% H_2S	Low / 10%	30	20	54.2	68.2	14.5	18.2
	High / 1.5%	30	20	61.6	80.7	17.0	22.3

From Figure 12 and Table 6 it can be concluded that humidity reduces the obtained CO_2 permeance at a relatively flat CO_2/CH_4 selectivity. After the feed flow rate increases, the H_2S permeance is not fully stabilized upon humidity removal, but its behavior seems unaffected by the presence of humidity in agreement with the results shown in the section 3.2 on self-standing CTA dense films. It seems relatively clear that the presence of humidity increases H_2S/CH_4 selectivity. Unfortunately, due to the limited gas inventory and specialized nature of these experiments, it is challenging to run at higher feed flow rates for longer duration. The

stability of CTA hollow fibers with H_2S and moisture is still worth investigating for potential industrial application.

4.3 Post-process analysis

To understand the differences (if any) caused by the humid sour gas mixture on CTA dense membranes, samples were analyzed by 3 different techniques: hydrogen nuclear magnetic resonance (^{1}H-NMR), thermo-gravimetrical analysis (TGA), and Fourier Transform Infrared Spectroscopy (FTIR). For the characterization by ^{1}H-NMR, around 10 mg of every film was dissolved in deuterated DMSO (d6-DMSO) and placed in a typical NMR tube to be analyzed in a C4315 - Bruker 400MHz device. The comparison of the samples analyzed is shown in the Appendix (Figure S1). In principle, no visual changes have been observed. To be more precise, the area of the cellulose ring (Figure S2) and the area of the substituted acetate (Figure S3) had been enlarged. No differences were found by ^{1}H-NMR. It can thus be concluded that the main part of the polymer film remained unchanged after being exposed to different gas feed conditions. A similar conclusion can be drawn from the analysis of the samples by thermogravimetric analysis (TGA) as shown in Figure S4. After a small initial weight loss, attributed to the water adsorbed in the film, the samples show the same weight loss pattern indicating that the majority of the structure shows similar thermal stability.

The surface of the films was subsequently analyzed by FTIR as is shown in Figure 13. The measurements were repeated 5 times to ensure reproducibility. It is important to understand if there is any interaction between the polymer matrix and the gases, especially H_2S and H_2O. For this reason, in Figure 14, the areas where possible interaction may happen (around 3600 cm^{-1}) are magnified. The enlarged area in Figure 14, an additional peak in the samples CTA#5, CTA#6 and CTA#7 in comparison to the sample CTA#3 can be observed. The area of this peak corresponds to the S-O bond stretching which can confirm the presence of sulfur molecules [21]. This may suggest that at least, the non-acetylated part of the cellulose triacetate structure may have been chemically altered where parts of the molecule would have changed. It is also possible to see in Figure 14 the differences between the sides of the film where the top part is more affected than the bottom part. This is a clear indication that the process occurring is related to the interaction or condensation of the humid gas on the feed side of the membrane.

Sample	Tested	Humidity	H_2S
CTA#3	30 °C, 20 and 50 bar	No humidity	15%
CTA#5	50 °C, 50 bar	Up to 1800 ppm	No H_2S
CTA#6	30 °C, 20 and 50 bar	Up to 1800 ppm	15%
CTA#7	30 and 50 °C, 20 bar	Up to 5000 ppm	15%

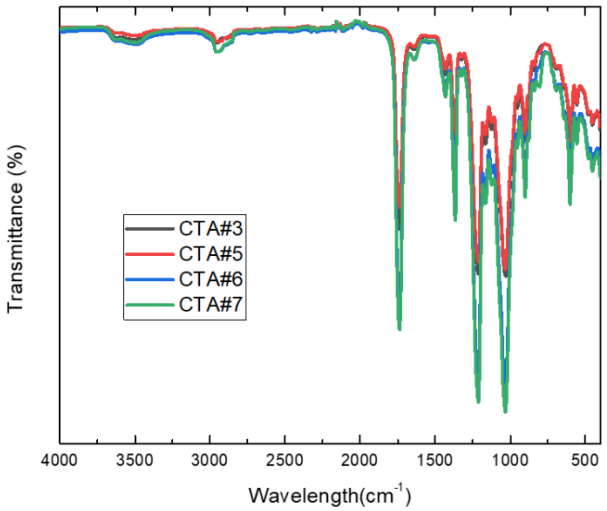

Figure 13 Conditions that the various CTA films have experienced (left), FTIR for the CTA films where CTA#3,6 and 7 where exposed to humidity and sour gas mixtures, whereas CTA #5 was only exposed to humidity but NOT the H_2S containing sour-gas mixture (right).

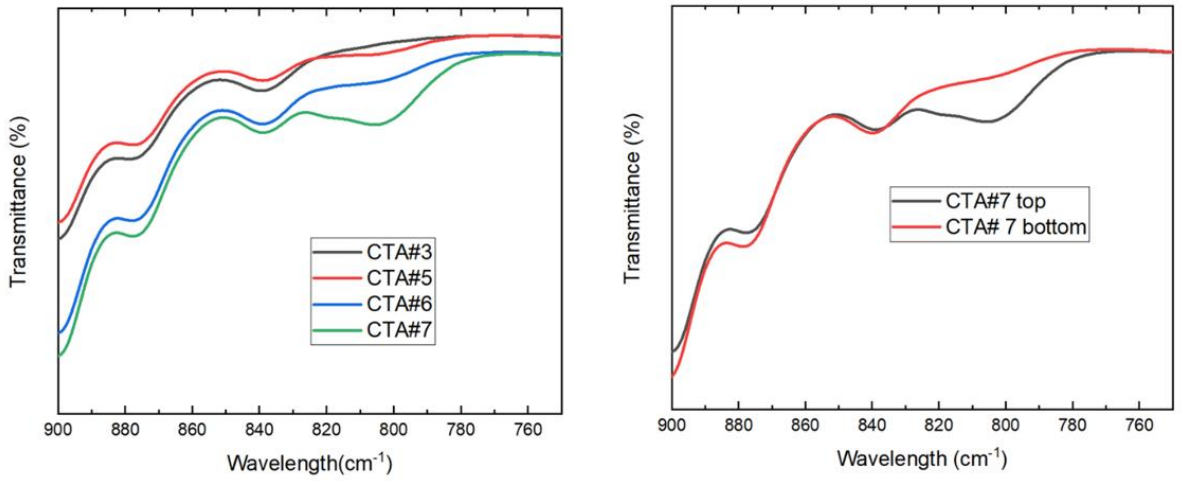

Figure 14 FTIR of the area where possible interaction with H_2S can be detected (left) and differences between the top and bottom parts of the films (right).

While the CTA#3 film showed great stability, the CTA#5, CTA#6 and CTA#7 showed the effect of the interaction of the polymer matrix with the gas in the feed side. This effect is more significant for samples CTA#5 and CTA#7. Especially interesting is the case of the sample CTA#5 which was not exposed to H_2S, but still showed degradation. It seems that the higher water content and temperature may act as a trigger for a substitution reaction. It can be observed from the TGA analysis shown in Figure S4 that the amount of condensed liquid in the membrane is around 0.5 wt. %. Since this effect amount is too small to be detected by ^{1}H-NMR, it confirms that the process may occur only on the surface of the film.

5 Conclusions

The current study aims to provide a thorough understanding of the separation performance of the cellulose (tri)-acetate (CTA) membrane material in humid high H_2S natural gas feed streams. The systematic study of the gas separation performances of CTA polymers has been carried out in self-standing symmetric films and asymmetric hollow fiber membranes. The separation performance in H_2S-containing mixtures ($CH_4/CO_2/H_2S$, 80/5/15) were evaluated at 30 and 50 °C at 20, 35 and 50 bar, including higher hydrocarbons in the presence of various levels of humidity, up to 4500 ppm or 80% RH, depending on conditions of temperature and pressure.

The introduction of butane and toluene in the high H_2S feed mixture resulted in an inhibition of both the CO_2 and H_2S permeability. Both the CO_2/CH_4 and H_2S/CH_4 selectivity were seemingly unaffected at these operating conditions (30 °C and 20 bar). In general, highly condensable gases with large kinetic sizes, such as toluene, compete with H_2S and CO_2 by sorption but can also hinder their diffusion. Therefore, at limited absolute pressure, a higher toluene partial pressure resulted in decreased H_2S/CH_4 and CO_2/CH_4 selectivities. Nevertheless, the controlled plasticization of the CTA membrane at elevated H_2S partial pressure created new free volume (sorption-favored) and passage (diffusion-favored) for all gas molecules. Potentially, the enhanced detrimental effect of toluene on the CTA performance at elevated pressure was offset by the new “opportunities” for permeation.

The addition of humidity resulted in a slight increase of both H_2S/CH_4 and CO_2/CH_4 selectivity at a minor decrease in both CO_2 and H_2S permeance. During the humid operation (40% RH and 80% RH), a 7-8% drop in CO_2 and H_2S permeance was observed. As the CH_4 permeance reduced to a larger extent, the CO_2/CH_4 and H_2S/CH_4 selectivity increased only marginally. After removal of the humidity, it can be concluded that the exposure to humidity reduced the obtained CO_2 permeance at a relatively flat CO_2/CH_4 selectivity. The H_2S permeance seemed unaffected by the presence of humidity, while it was observed that humidity presence slightly increased H_2S/CH_4 selectivity.

Our hypothesis is in the higher H_2S environment, the combination of H_2S plasticizing and hydrophilic nature of CTA enables the swelling of polymer chains which allows the H_2S molecules to pass through, but there is still significant competitive sorption between condensable gases (H_2S, CO_2 and H_2O) versus CH_4 which helps in preserving or slightly

increasing selectivity. H_2S separation behavior seems to be benefit from the presence of high moisture content.

To understand any chemical changes due to humid sour gas exposure, the CTA films have been characterized using various analytical techniques. 1H-NMR showed no significant differences and TGA showed similar thermal stability of the CTA films before and after the sour gas exposure. FTIR showed differences for the sample CTA#5, CTA#6 and CTA#7 compared to CTA#3 probably due to the condensation of acidified water on top of the film due to the larger water content and temperature. This effect was especially significant on the sample CTA#7.

For the first time, the effect of these contaminants and humidity together has thus been evaluated. By careful time-based permeation study of CTA membranes at various pressures, temperatures, and different gas mixtures of sour gas (15% H_2S) with heavy hydrocarbons (up to butane, toluene) and up to high levels of humidity it is evident to say the membrane stability (both permeability and selectivity) is promising. With the improvement of permeability due to combination of H_2S plasticization and competitive sorption, this phenomenon is attractive and worth studying further.

Acknowledgements

The authors gratefully acknowledge the financial support by Chevron Energy Technology Company (Contract No. CW1804561).

References

[1] A. Kidnay, W. Parrish, Overview of natural gas industry, *Fundam. Nat. Gas Process. CRC Press, Taylor & Francis Group, Boca Raton, FL*, (2006) 1-21.
[2] Y. Alcheikhhamdon, M. Hoorfar, Natural gas quality enhancement: A review of the conventional treatment processes, and the industrial challenges facing emerging technologies, *Journal of Natural Gas Science and Engineering*, 34 (2016) 689-701.
[3] Y. Alcheikhhamdon, M. Hoorfar, Natural gas purification from acid gases using membranes: A review of the history, features, techno-commercial challenges, and process intensification of commercial membranes, *Chemical Engineering and Processing - Process Intensification*, 120 (2017) 105-113.
[4] N. Bhuwania, S. Husain, D. Chinn, R.P. Macdonald, T.K. Das, Systems and methods to manage heat in an integrated oil and gas processing plant with sour gas injection, US Patent 10,905,996, Chevron USA Inc., 2021.
[5] D. Chinn, N. Bhuwania, S. Husain, R.P. Macdonald, T.K. Das, Systems and methods to debottleneck an integrated oil and gas processing plant with sour gas injection, US Patent 10,363,518, Chevron USA Inc., 2019.

[6] N. Bhuwania, S. Husain, D. Chinn, R.P. Macdonald, T.K. Das, Systems and methods to dehydrate high acid gas streams using membranes in an oil and gas processing plant, US Patent 10,363,517, Chevron USA Inc., 2019.
[7] Y. Chu, X. He, Process Simulation and Cost Evaluation of Carbon Membranes for CO2 Removal from High-Pressure Natural Gas, *Membranes*, 8 (2018) 118.
[8] Y. Liu, Z. Liu, A. Morisato, N. Bhuwania, D. Chinn, W.J. Koros, Natural gas sweetening using a cellulose triacetate hollow fiber membrane illustrating controlled plasticization benefits, *Journal of Membrane Science*, 601 (2020) 117910.
[9] Y. Liu, Z. Liu, G. Liu, W. Qiu, N. Bhuwania, D. Chinn, W.J. Koros, Surprising plasticization benefits in natural gas upgrading using polyimide membranes, *Journal of Membrane Science*, 593 (2020) 117430.
[10] A. Morisato, E. Mahley, Hydrogen sulfide permeation and hydrocarbon separation properties in cellulose triacetate hollow fiber membrane for high hydrogen sulfide contained natural gas sweetening applications, *Journal of Membrane Science*, 681 (2023) 121734.
[11] H.T. Lu, S. Kanehashi, C.A. Scholes, S.E. Kentish, The impact of ethylene glycol and hydrogen sulphide on the performance of cellulose triacetate membranes in natural gas sweetening, *Journal of Membrane Science*, 539 (2017) 432-440.
[12] C.S.K. Achoundong, N. Bhuwania, S.K. Burgess, O. Karvan, J.R. Johnson, W.J. Koros, Silane modification of cellulose acetate dense films as materials for acid gas removal, *Macromolecules*, 46 (2013) 5584-5594.
[13] N.N. Li, E.W. Funk, Y.A. Chang, S.S. Kulkarni, A.X. Swamikannu, L.S. White, Membrane separation processes in the petrochemical industry, in, United States, 1987.
[14] C.A. Scholes, S. Kanehashi, Polymeric membrane gas separation performance improvements through supercritical CO2 treatment, *Journal of Membrane Science*, 566 (2018) 239-248.
[15] G. Genduso, I. Pinnau, Quantification of sorption, diffusion, and plasticization properties of cellulose triacetate films under mixed-gas CO2/CH4 environment, *Journal of Membrane Science*, 610 (2020) 118269.
[16] R. Swaidan, B. Ghanem, M. Al-Saeedi, E. Litwiller, I. Pinnau, Role of Intrachain Rigidity in the Plasticization of Intrinsically Microporous Triptycene-Based Polyimide Membranes in Mixed-Gas CO2/CH4 Separations, *Macromolecules*, 47 (2014) 7453-7462.
[17] M.R. Kosuri, W.J. Koros, Defect-free asymmetric hollow fiber membranes from Torlon®, a polyamide–imide polymer, for high-pressure CO2 separations, *Journal of Membrane Science*, 320 (2008) 65-72.
[18] D.W. Wallace, C. Staudt-Bickel, W.J. Koros, Efficient development of effective hollow fiber membranes for gas separations from novel polymers, *Journal of Membrane Science*, 278 (2006) 92-104.
[19] O. Karvan, J.R. Johnson, P.J. Williams, W.J. Koros, A Pilot-Scale System for Carbon Molecular Sieve Hollow Fiber Membrane Manufacturing, *Chemical Engineering & Technology*, 36 (2013) 53-61.
[20] S.J. Kim, J.W. Lee, S.Y. Nam, Fabrication of Cellulose Triacetate Hollow Fiber Membranes for Forward Osmosis-Nanofiltration, *J Nanosci Nanotechnol*, 18 (2018) 6180-6188.
[21] H. He, C.-G. Zhang, J.-L. Xia, A.-A. Peng, Y. Yang, H.-C. Jiang, L. Zheng, C.-Y. Ma, Y.-D. Zhao, Z.-Y. Nie, G.-Z. Qiu, Investigation of Elemental Sulfur Speciation Transformation Mediated by Acidithiobacillus ferrooxidans, *Current Microbiology*, 58 (2009) 300-307.

Appendix

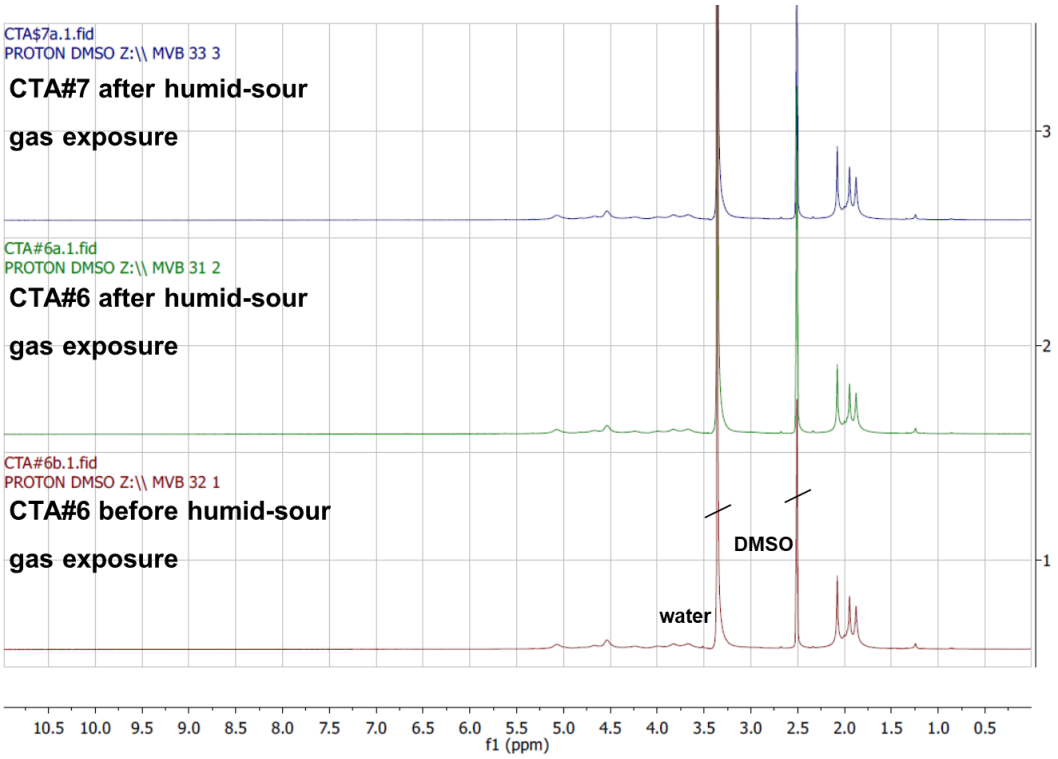

Figure S1. [1]H-NMR for the CTA films before and after measurement under H_2S and humid conditions.

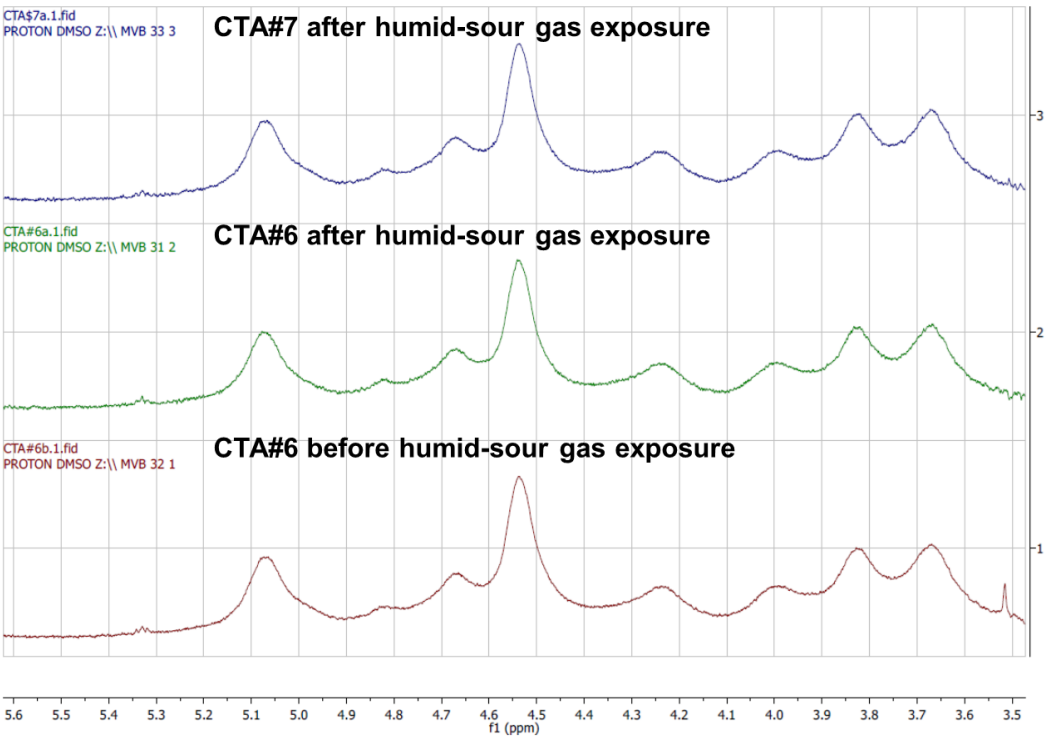

Figure S2: [1]H-NMR for the CTA films before and after measurement: enlargement of the cellulose ring area.

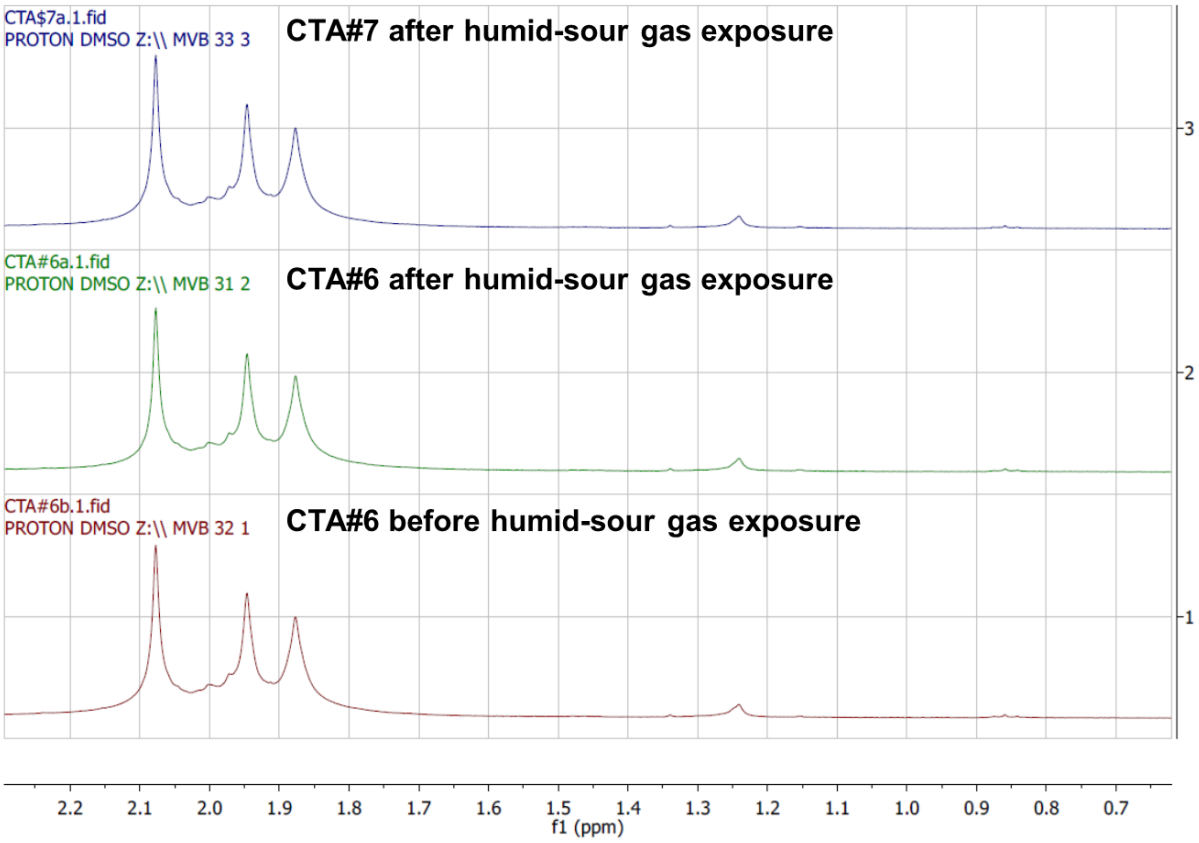

Figure S3: [1]H-NMR for the CTA films before and after measurement: enlargement of the acetate substituted area.

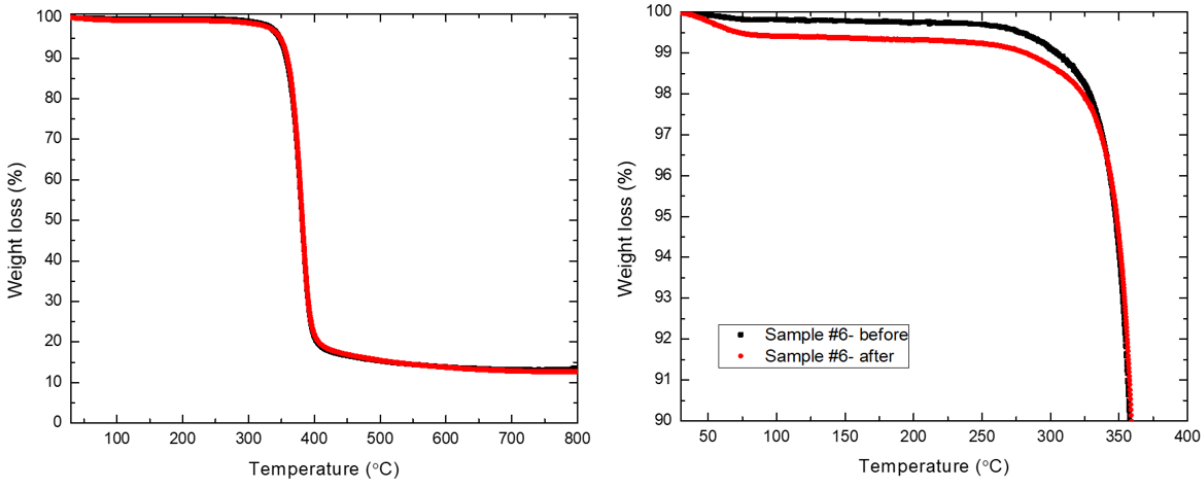

Figure S4: TGA of the CTA films

Declaration of interests

☒ The authors declare that they have no known competing financial interests or personal relationships that could have appeared to influence the work reported in this paper.

☐The authors declare the following financial interests/personal relationships which may be considered as potential competing interests: